QUALITATIVE ANALYSIS OF THE DYNAMIC CRACK INITIATION AND PROPAGATION

M. Watanabe

JOURNAL DE PHYSIQUE IV
Colloque C3, suppl. au Journal de Physique III, Vol. 1, octobre 1991

QUALITATIVE ANALYSIS OF THE DYNAMIC CRACK INITIATION AND PROPAGATION

M. WATANABE

Kinki University, Faculty of Engineering, Umenobe, Takaya, Higashi-Hiroshima 729-17, Japan

résumé: Des résultats expérimentaux de fissuration rapide sont analysés à partire de l'équation de conservation de l'energie prenant en compte l'effet de microcavités générées au sommet de la fissure. Le rayon moyen des microcavités est supposé croître selon une loi de puissance t^{α} et le volume des microcavitésest défini par r^{D} et leur densité de distribution par $r^{-\beta}$. les valeurs de α sont estimées en fonction de celles de β. La rugosité de surface peut être analysée qualitativement à partir de la détermination expérimentale des paramètres D et β. La condition postulée d'incitation de la fissure est étendue à la phase de propagation. Les résultats sont en accord qualitatif avec les expériences.

Abstract-Experimental results of the fast fracture of the crack is analyzed based on the extended energy balance equation in which the effect of microvoids generated at the tip of the crack is taken into account. We assume that the average radius r of microvoids grow in time as $r \propto t^{\alpha}$, i.e., microvoids grow in the self-similar manner, statistically. It's volume is defined as r^{D} and the density distribution function n(r) of the microvoids is assumed to be $n \propto r^{-\beta}$, where D and β are numbers. The surface roughness $\langle r \rangle$ defined as the average radius of microvoids is compared with the experiment. Thus we can estimate the numbers α and β as $\alpha \fallingdotseq 5.5$ for $1 > \beta > 0$ and $\alpha > 5.5$ for $2 > \beta > 1$, respectively. We have shown that the surface roughness which is called as "mirror", "mist" and "hackle" can be qualitatively analyzed from the energy balance equation if the parameters D and β are measured experimentally. Furthermore, we have postulated the initiation condition of the dynamically loaded crack and extended it to the propagation stage. This postulate and it's extension show the qualitative agreement with the experimental observations.

I. Introduction.

We analyze the results of the series of the experiments on the fast fractute performed by Ravi-Chandar and Knauss /1/. The specimen material used in their experiment is Homalite 100 and it's size is chosen such that the reflected waves do not interact with the crack tip for the duration of the experiment and thus a literally unbounded (plate) medium is simulated. They applied the tensile stress using the electromagnetic loading device and measured the stress intensity factor history by the method of caustics. Investigating various different aspects of the dynamic fracture, they found that crack propagation occurs by the linking up of many microvoids(or microcracks). Our analysis is based on this observation and the assumption that microvoids grow in the self-similar manner statistically.

II. The growth law and the density of the microvoids.

The micromechanics of rupture of polymers under tensile stress was thoroughly investigated /2/. For example, physical mechanism of the generation of microvoids is clarified in the frame work of thermal activation theory of fracture of solids. Zhurkov and Kuksenko /3/ propposed the hypothesis that the formation and development of microvoids (or submicrocracks) play a dominant role in the micromechanics of fracture of polymers. They measured the microvoid distribution in the direction of the crack growth as shown in Fig. 1 by the small angle X-ray scattering. They also compared the scattering curves during the initial stage of fracture long before rupture, to scattering before rupture and found the significant changes in the sizes of microvoids. The enelarged microvoids are regarded as the coalescence of the primary microvoids.

In the experiment of the dynamic fracture, Ravi-Chander and Knauss found that crack propagation occurs by the linking up of many microvoids(or microcracks). The number of growing microvoids that are activated is a function of the stress intensity factor and the distribution of voids in the material itself. The fractured surface depth d is measured along the crack path and it's variation is shown as a function of the measured stress intensity factor. They established a quantitative correlation between the stress intensity factor and the surface roughness as shown in Fig. 2. We find the following relation from Fig. 2

$$\frac{d}{d_{max}} = \left(\frac{K_I}{K_0}\right)^{11.1} \qquad (1)$$

where K_I is the stress intensity factor and K_0 is a constant.

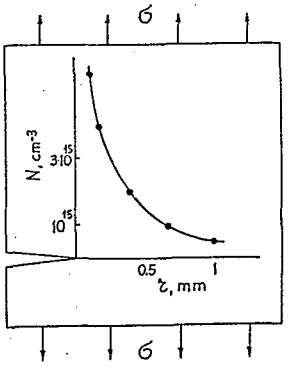

Fig. 1. Microvoid distribution in the direction of the crack growth /3/.

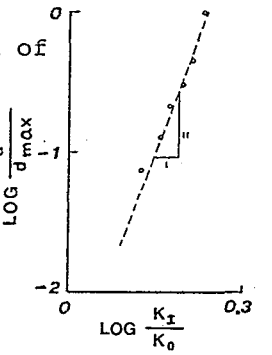

Fig. 2. Variation of the size of the fracture process zone with crack extension and stress intensity factor /1/.

The diameters of the microvoids measured in the static case range from 0.009 to 0.3 μm for different polymers /3/. When the applied stress is sufficiently small, the radius r_0 of the microvoid is determined by the thermal equilibrium condtion. In the dynamic case, the size of the microvoids increases by various different mechanisms as the stress intensity factor increases. Finally the microvoid grow to be a small microcrack whose length reaches to the range of milimeter. We assume that the characteristic length of the microvoids does not exist in these growth processes. In such situations, the microvoids grow in the self-similar manner statistically /4/ and the radius r of the microvoids can be assumed as

$$r = r_0 \left(\frac{t}{t_0}\right)^{\alpha}, \qquad (2)$$

where t_0 is a characteristic time for generation of microvoids in thermal equilibrium. The growth rate of the microvoid is determined by the number α. As the crack propagates, the microvoids near the tip of the crack is activated. Suppose that the microvoids start to grow when the distance between the crack and the microvoids becomes R. In this case, the following relation holds

$$\frac{K_I}{\sqrt{2\pi R}} = \sigma_c, \qquad (3)$$

where the quantity σ_c is the average critical stress for the growth of the microvoids. Since the crack propagates by the constant velocity $\dot{a}$ /1/, the interaction time τ_{int} between the crack and the microvoids can be obtained by

$$\tau_{int} = \frac{R}{\dot{a}} = \frac{K_I^2}{2\pi\sigma_c^2 \dot{a}} \tag{4}$$

The maximum radius r_m of the microvoids in the fractured surface can be expressed as

$$r_m = r_0 \left(\frac{R}{\dot{a} t_0}\right)^{\alpha} = r_0 \left(\frac{K_I^2}{2\pi\sigma_c^2 \dot{a} t_0}\right)^{\alpha} \tag{5}$$

The interaction time τ_{int} between the crack and the microvoids changes due to the shielding effect associated with the inhomogenuity of the specimen and other reasons which is not discussed here. Thus the microvoids with various different radius are produced. We assume the density distribution function of the microvoids as

$$n = n_0 (r_0 / r)^{\beta} \tag{6}$$

where n_0 is the density of microvoids in thermal equilibrium.

The average radius $\langle r \rangle$ of the microvoids in the fractured surface can be defined as

$$\langle r \rangle = \int_{r_0}^{r_m} r\, n(r)\, dr \Big/ \int_{r_0}^{r_m} n(r)\, dr \tag{7}$$

The average radius $\langle r \rangle$ of the microvoids is regarded as the quantity which is proportional to the surface roughness d / d_{max} defined by Eq. (1), The K_I dependence of the average radius $\langle r \rangle$ can be found in the following

$$\langle r \rangle = \frac{1-\beta}{2-\beta} r_m = \frac{1-\beta}{2-\beta} r_0 \left(\frac{K_I^2}{2\pi\sigma_c^2 \dot{a} t_0}\right)^{\alpha} \qquad \text{for } 1 > \beta > 0$$
$$\propto K_I^{1.5} \qquad \therefore \ \alpha \approx 5.5 \tag{8}$$

$$\langle r \rangle = \frac{\beta-1}{2-\beta} r_0 \left(\frac{r_m}{r_0}\right)^{2-\beta} = \frac{\beta-1}{2-\beta} r_0 \left(\frac{K_I^2}{2\pi\sigma_c^2 \dot{a} t_0}\right)^{\alpha(2-\beta)} \qquad \text{for } 2 > \beta > 1$$
$$\propto K_I^{1.5} \qquad \therefore \ \alpha(2-\beta) \approx 5.5 \tag{9}$$

where $r_0 / r_m \ll 1$ is used. In the latter case, we find $\alpha > 5.5$ from the condition $2 > \beta > 1$. If $\beta = 1$ or $\beta = 2$, the average radius $\langle r \rangle$ depends on $\ln(r_m / r_0)$, which is not observed in the experiment. In the case $\beta > 2$, we find $\langle r \rangle = (\beta - 1) r_0 / (\beta - 1)$ which is independent of K_I. Thus we have disregarded these cases. The average density $\langle n \rangle$ defined by

$$\langle n \rangle = \int_{r_0}^{r_m} n(r)\, dr \Big/ \int_{r_0}^{r_m} dr \tag{10}$$

plays an important role in considering the behavior of the microvoids. In D dimensional space the average distance between microvoids is given by $\langle n \rangle^{-1/D}$. When the average radius $\langle r \rangle$ of the microvoids reaches the distance $\langle n \rangle^{-1/D}$, microvoids coalesce with each other. In Table 1, we show the values of the quantities $\langle n \rangle / n_0$ and $\langle n \rangle \langle r \rangle^D / (n_0 r_0^D)$

Table 1.

	$\beta > 2$	$\beta = 2$	$2 > \beta > 1$	$\beta = 1$	$1 > \beta > 0$
$\langle n \rangle / n_0$	$\frac{r_0}{(\beta-1) r_m}$	$\frac{r_0}{r_m}$	$\frac{r_0}{(\beta-1) r_m}$	$\frac{r_0}{r_m} \ln\left(\frac{r_m}{r_0}\right)$	$\frac{1}{1-\beta}\left(\frac{r_0}{r_m}\right)^{\beta}$
$\frac{\langle n \rangle \langle r \rangle^D}{n_0 r_0^D}$	$\frac{(\beta-1)^D r_0}{(\beta-2)^D r_m}$	$\frac{r_0}{r_m}\left(\ln\frac{r_m}{r_0}\right)^D$	$\frac{(\beta-1)^{D-1}}{(2-\beta)^D}\left(\frac{r_0}{r_m}\right)^{D(\beta-2)+1}$	$\frac{\frac{r_m}{r_0}}{\left(\ln\frac{r_m}{r_0}\right)^{D-1}}$	$\frac{(1-\beta)^{D-1}}{(2-\beta)^D}\left(\frac{r_m}{r_0}\right)^{D-\beta}$

We find from Table 1 that the average number $\langle n \rangle$ of the microvoid decreases as the microvoids grow due to the coalescence among them. The value of $\langle n \rangle \langle r \rangle^D$ decreases for $\beta \geqq 2$, while it could increase if $\beta < 2$. These conditions are closely related with the branching and will be discussed in the next section.

III. The dynamic crack propagation and the branching.

When the stress intensity factor is not so large in compared with K_{IC} and the crack velocity is relatively small, say = 240 m/s, the energy balance equation of Griffith can be applied

$$(1 - \frac{\dot{a}}{c_R}) G^* = 2\gamma_0 \qquad (11)$$

where c_R is the velocity of the Rayleigh wave and G^* the "static" energy release rate. In this case the quasi-static condition is satisfied and the effect of the term ( ) in L.H.S. of Eq. (11) is observed /1/, /5/. The fractured surface is smooth and is characterized as the "mirror" state. As the stress intensity factor increases the fractured surface changes from "mirror" to the "mist" or "hackle" state. In this case, the additional energy which is absorbed by the microvoids should be added in Eq. (11),

$$(1 - \frac{\dot{a}}{c_R}) G^* w \, da = 2\gamma_0 w \, da + \gamma_0 \sum_i \Delta S_i \qquad (12)$$

The quantity ΔS_i represents the increased area of the microvoid during the period of t and t+dt. ΔS_i can be written as $\Delta S_i \approx c_i (D_i - 1) r_i^{D_i - 2} dr_i$, where r_i and D_i are the radius and the spacial dimension of the i-th microvoid, respectively. The quantity w is the width of the specimen. Making use of Eq. (2), we find

$$dr = \frac{\alpha r_0}{t_0} (\frac{r}{r_0})^{1 - (1/\alpha)} \, dt \qquad (13)$$

Eq. (13) is used in calculating the averaged quantities of ΔS_i. The microvoid is generated in the small volume $\Delta V = w R \langle r \rangle$, and the average number of the microvoids can be written as $\langle n \rangle \Delta V$. Thus the second term in R.H.S. of Eq. (12) can be written as

$$\gamma_0 \sum_i \Delta S_i = \gamma_0 \langle n \rangle \Delta V \frac{\alpha r_0^{1/\alpha}}{t_0} (D - 1) c \langle r^{D - 1 - (1/\alpha)} \rangle \, dt \qquad (14)$$

where c is a constant and D the average spacial dimension of the microvoids. In calculating the quantity $\langle r^{D - 1 - (1/\alpha)} \rangle$, we have to divide it into numerous different cases. If the condition $1 > \beta > 0$ is satisfied, Eq. (12) can be written as

$$(1 - \frac{\dot{a}}{c_R}) G^* - 2\gamma_0$$

$$= \gamma_0 \frac{\alpha^2 (1 - \beta)(D - 1) c}{(2 - \beta)\{\alpha (D - \beta) - 1\}} n_0 r_0^D (\frac{\tau_{int}}{t_0})^{\alpha (D - \beta)}$$

$$= \gamma_0 \frac{(2 - \beta)^{D-1} \alpha^2 (D - 1) c}{(1 - \beta)^{D-2} \{\alpha (D - \beta) - 1\}} \langle n \rangle \langle r \rangle^D \qquad (15)$$

Substituting the numbers $\alpha = 5.5$ and $\beta = 0.7$, we find

R.H.S. of Eq. (15) / $\langle n \rangle \langle r \rangle^D \approx 630 \gamma_0$ for D = 3, $c = 4\pi$ and $\approx 40 \gamma_0$ for D = 2, $c = 2\pi$.

The condition $\langle n \rangle \langle r \rangle^3 \approx 1$ yields $\tau_{int} / t_0 \approx (25 / n_0 r_0^3)^{1/13}$ for the former and $\tau_{int} / t_0 \approx (5.6 / n_0 r_0^2)^{1/7.2}$ for the latter case. Thus the surface roughness can be qualitatively analyzed from the energy balance equation if one measures the parameters such as D and β besides the measurement shown in Fig. 2. Since the numerical factor in R.H.S. of Eq. (15) is rather large in compared with $2\gamma_0$, the branching condition will be given by the numerical value of $\langle n \rangle \langle r \rangle^D$ and it probably lies within the inequqlitities $10 > \tau_{int} / t_0 > 1$. This condition can be expressed by the stress intensity factor using Eq. (4). Since the condition $\langle n \rangle \langle r \rangle^D \approx 1$ will not be satisfied for $\beta \geqq 2$ provided $n_0 r_0^D \ll 1$, we disregard these cases. The energy balance equation for $2 > \beta > 1$ is

$$\left\{(1-\frac{\dot{a}}{c_R})\,G^{*}-2\gamma_0\right\}=\gamma_0\frac{\alpha^2 c\,(D-1)\,(2-\beta)^{D-1}\langle n\rangle\langle r\rangle^{D}}{(\beta-1)^{D-2}\{\alpha\,(D-\beta)-1\}}\left(\frac{\tau_{int}}{t_0}\right)^{\alpha(\beta-1)(D-2)}\quad\text{if}\quad\alpha\,(D-\beta)\rangle 1 \qquad (16)$$

Substituting the numbers $\alpha = 7$ and $\beta = 1.3$ as an example we find

$$\left\{(1-\frac{\dot{a}}{c_R})\,G^{*}-2\gamma_0\right\}/\langle n\rangle\langle r\rangle^{D}\approx 180\,\gamma_0\left(\frac{\tau_{int}}{t_0}\right)^{2.1}\quad\text{for } D=3,\ c=4\pi \text{ and } \approx 55\,\gamma_0 \text{ for } D=2,\ c=2\pi \qquad (17)$$

The condition $\langle n\rangle\langle r\rangle^{D}\approx 1$ yields $\tau_{int}/t_0\approx(4/n_0 r_0^3)^{1/7.7}$ for the former and $\tau_{int}/t_0\approx(2/n_0 r_0^2)^{1/2.8}$ for the latter case. These numerical examples lead to the similar conclusion to the case $1 \rangle \beta \rangle 0$.

IV. The dynamic crack initiation.

Ravi-Chander and Knauss /1/ found the time dependence of the critical stress intensity factor K_{IC} for crack initiation as shown in Fig. 3. In the quasi-static condition, the crack start to propagate if the condition $K_{IC} = K_C$ is satisfied. This condition is equivalent to the energy balance equation $G^{*}=2\gamma_0$. The experimental observation $K_{IC} \propto t^{-2}$ for $t \leq 50\ \mu s$ indicates that the additional condition for the dynamic crack initiation is required, which is different from the quasi-static energy balance equation. In order to explain the dynamic crack initiation shown in Fig. 3, we postulate the following condition for the crack initiation.

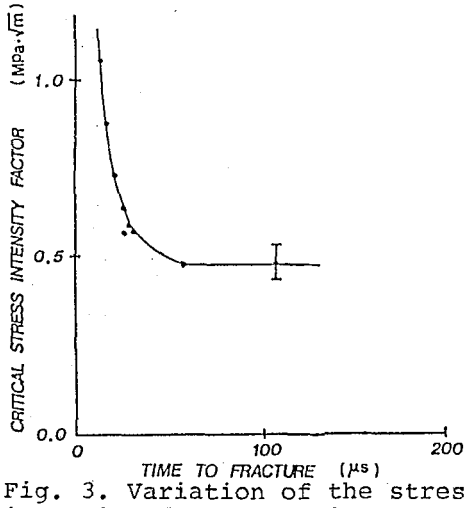

Fig. 3. Variation of the stress intensity factor required for initiation with time to fracture/1/

$$S = S_C \qquad (18)$$

where S is the surface area fractured at the tip of the crack and S_C is the critical surface area for the crack initiation. The surface area S increases in time and it's time dependence is assumed to be

$$S(t) = S_1\left(\frac{t}{t_1}\right)^{\alpha_s} \qquad \text{for } t \leq t_1 \qquad (19)$$

where $S_1 = w R_{IC}$ and $t_1 = 50\ \mu s$ from Fig., 3 and α_s is the number. The quantities R_{IC} and $R_C = S_C / w$ are defined as

$$\frac{K_{IC}}{\sqrt{2\pi R_{IC}}}=\sigma_C\ ,\qquad \frac{K_C}{\sqrt{2\pi R_C}}=\sigma_C. \qquad (20)$$

Suppose that the crack start to grow with $t \langle 50\ \mu s$. In this case we find the following equation

$$S_1\left(\frac{t}{t_1}\right)^{\alpha_s}=w R_C \qquad \therefore\quad R_{IC}=R_C\left(\frac{t_1}{t}\right)^{\alpha_s}. \qquad (21)$$

Eq. (21) can be written as

$$K_{IC}^2=K_C^2\left(\frac{t_1}{t}\right)^{\alpha_s}, \qquad (22)$$

which determines the effective surface energy $2\gamma(t)$ such that the energy balance equation $G^{*}=2\gamma(t)$ holds. Comparing Eq. (22) with Fig. 3, we find $\alpha_s = 4$. Note here that the quasi-static initiation of the crack is included in Eq. (22) if one sets $t = t_1$ and $\gamma = \gamma_0$. in the energy balance equation.

Fig. 4 shows the stress intensity factor and the crack extension history /1/. They observe that the arrival of the wave reflected from the boundaries at about 150 μs causes the stress intensity factor to increase as in Fig. 4 (solid line) and the crack velocity changes from 240 m/s to 350 m/s. They conclude from these observations that

crack travling at a low velocities, typically below 300 m/s, can change their velocity of propagation upon encounter ing str ess waves.

According to the postulate shown in Eqs. (18) and (19), the crack starts to propagate at $S = S_C$ and the crack velocity is determined by the following equation

$$\dot{a} = \frac{1}{w}\left(\frac{dS}{dt}\right)_{S=S_C} = \left(\frac{\alpha_S}{t} + \frac{2}{K_{IC}}\frac{dK_{IC}}{dt}\right) S_C \quad (23)$$

The crack velocity is determined by the initiation condition of the crack which consist of the two terms of ( ) in R.H.S. of Eq. (23). The former shows the characteristic time of the growth of S(t) , while the latter is associated with the dynamic behavior of the stress intensity factor at the initiation. Once the crack starts to propagate, we do not have to restrict these two terms at the initiation. Thus we can replace $K_{IC}(t)$ by $K_I(t)$ in Eq. (23). Numerical evaluation of the two terms in R.H.S. of Eq. (23) indicates that the first term is always larger than the second term except at encountering the stress wave. When the crack encounters with the stress wave at t = 150 μs (solid line of Fig. 4), we find

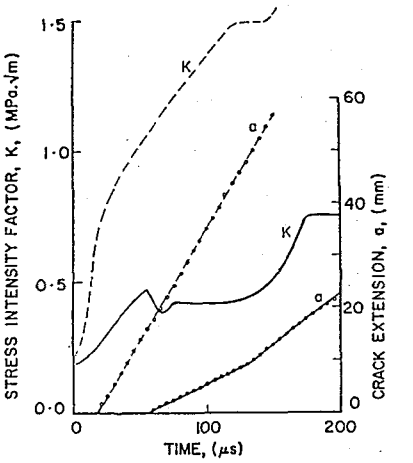

Fig. 4 Stress intensity factor and crack extension history/1/

$$\frac{1}{K_I}\frac{dK_I}{dt} \geq \frac{\alpha_S}{t} \quad (24)$$

When the crack encounters with the stress wave, the experimental observation indicates that the characteristic time of the growth of S(t) changes and remains unchanged there after. In order to clarify the theoretical r easons for it, one has to look into the the atomic motion of the mater ial which is beyond the scope of this work.

V. Conclusion.

We have assumed that the fr acture proceeds in the self similar manner statistically. Based on this assumption we have estimated the surface roughness associated with the micr ovoid growth and compared with the experiment /1/. Qualitative agreement between our analysis and the experimental observation shown in Eq. (1) demonstrates the importance of the par ameters α , β and D which could be determined by the experiment.

We have also postulated the initiation condition of the crack grow th which deter mines the effective surface energy $2\gamma(t)$ so that the energy balance equation also holds. Making use of this postulate we co uld explain the experimental obser vation of $K_{IC} \propto t^{-2}$. Extending this postulate to the propagation stage and evaluating the char acteristic time t and time derivative of $K_I(t)$ from Fig. 4, we could explain the dynamic behavior of the crack velocity when it encounters with the stress wave.

References

/1/ Ravi-Chander, K. and and Knauss, W.G. International J. of Fracture 25 (1984) 247, 26 (1984) 65, 141, 189

/2/ Yokobori,T. and Narisawa, I. "The strength of the polymer materials", Ômu-sha 1982 (in Japanese)

/3/ Zhurkov, S.N. and Kukshenko, V.S., International J. of Fr acture Mechanics 11 (1975) 629

/4/ See for example, Fur ukawa, H., Advances in Physics 34 (1985) 703

/5/ Ravi-Chandar, K. and Knauss, W.G., Trans. of ASME 54 (1987) 72